A Quantitative Analysis of a Non-Eruptive Volcanic Event: Mt. Spurr, Alaska, 2002-2006

David Mercier

Thesissubmitted to the faculty of the Virginia Polytechnic Institute and State University
in partial fulfillment of the requirements for the degree of

Master of Science
in
Geosciences

Robert P.Lowell, Chair
John A.Hole
EstebanGazel

29 Jan 2014
Blacksburg, VA

Keywords: Hydrothermal, Mt. Spurr, Unrest, Volcano

A Quantitative Analysis of a Non-Eruptive Volcanic Event: Mt. Spurr, Alaska, 2002-2006

David Mercier

ABSTRACT

Mt. Spurr is a volcano in proximity to Anchorage, Alaska and major airline routes making an eruption or episode of unrest potentially hazardous. Between 2004 and 2006, Mt. Spurr underwent such an episode of unrest involving increased seismic activity, CO_2 emissions, ice melting, and debris flows, which was likely forecasted by the increased seismicity of Oct 2002. The timeline of events provide data to construct a model analyzing the thermal energy release and constraining subsurface magmatic and hydrothermal processes during the period of unrest. The results show that the ice cauldron formation and the increase of meltwater temperature could not have been caused by the observed CO_2 release alone and suggest that enhanced hydrothermal heat transfer related to increased CO_2 output could provide the thermal power necessary to drive the melting event. Scaling hydrothermal convection in terms of its Rayleigh number and using boundary layer analysis suggests that the mean permeability of the volcanic edifice prior to the unrest event was $\sim 10^{-14}$ m^2. CO_2 release, most likely related to mechanical fracturing of the edifice by over-pressurized fluids at depth and signaled by increased seismicity likely enhanced the hydrothermal Rayleigh number and heat output by a combination of heating and increased permeability.

Acknowledgements

I would like to thank the Science Department at Concord University, more especially to my advisor there, Dave Matchen, for proper guidance, support, instruction, nudging, and counsel, without which I would never have seen the halls of a graduate school.

I would like to thank Virginia Tech for giving me the opportunity to be a Master's Student here. Thank you to Nancy Ross and the Department of Geosciences for their offerings of a Teaching Assistantship which I thoroughly enjoyed each semester, learning from my students as well as teaching them, and for the Tillman Scholarship I received because of it.

I am grateful for the summer support, in my first year, received from NASA grant NNX10AO38G to Robert P. Lowell.

A very special thank you to Matt Mikulich for his donations to Virginia Tech, making the Matthew J. Mikulich Endowed Scholarship in Geophysics possible; your scholarship was a great help to me in a time of need. Thank you for your continued support of Geophysics at Virginia Tech, and the assistance you give to students who are complete strangers to you; it is obvious that "ut prosim" is not simply a motto to you, but true words to live by.

A special thanks to Linda Bland, Connie Lowe, Ellen Mathena, Mary McMurray, and Jo Thomason, not only for all their help with proper forms and documentation, their candid conversations, and assistance with things never meant to be in their job description, but also for their alerting us grad students to the presence of free food located at various places on the fourth floor. A very special thank you to Connie Lowe, I can't thank you enough for your support, advice, stern advice when needed, and anecdotes

through the thin and thick of my times here at Virginia Tech; few people here at Tech know me the way you do, somehow I feel like I should apologize, ha ha ha. Your tireless support and efforts of selflessness go above and beyond that which I expected from your office, and which I can only repay in gratitude, your memory will live long with me.

Thank you to Jim Langridge, and Mark Lemon for fixing my undue share of computer connection issues; and to Fred and Drema, two of my favorite housekeeping people, always worthy of a conversation or welcomed, lengthy how do you do in the morning. I would like to thank Izzy and Lindsey, my Americano dealers at Seattle's Best, and the Underground in Blacksburg.

A sincere and heartfelt thank you goes to my family for their undying level of support through every twist and turn that my life has taken. My belief in being self-sustaining, I have had the unfortunate task of calling upon them for assistance, and true as family can be, they have been there for me. I love you all, thank you.

A special thanks to my fellow grad students, my office mates, my dinner party and game night friends, my few times I've attended trivia night pals, and especially those who delight in food. You have all had an effect on me in varying degrees, some of you have surprised me, and so I thank all of you, more particularly, Aida Farough, Josh Valentino, Kannikha Kolandaivelu, Kathy Davenport, Pavithra Sekhar, and Shreya Singh.

I would like to thank the many faculty members that I have learned so much from, whether in the class room or through impromptu meetings. You have been mindful of my education, for which I am thankful, and given selflessly to fulfill my inquiries both academic and professional, and so I thank: Bob Bodnar, John Chermak, Brian Romans, and Maddy Schreiber. Inclusive of the former group, and yet in a group all their own is

my committee: my advisor and hydrothermal geophysicist, Bob Lowell, seismologist, John Hole, and volcanic geochemist, Esteban Gazel, you have all been available for me and made the culmination of my thesis writing possible.

I offer a very special thanks to my advisor Bob Lowell. Without you, I may not have even been selected at Virginia Tech; it was your initiative and faith in me that got me here. You have been ever so patient, and prodding when need be, through the ups and downs of my personal and academic life. Your advices have been well taken, and I can only say that I should have spent more time in your office than I did. I hope I have not let you down, and I thank you immensely for the opportunity you gave me here at Virginia Tech.

Table of Contents

List of Figures

List of Tables

1. Introduction

Eruptive events can cause hazards such as ash plumes, massive degassing, and debris flows which may contain large volumes of meltwater. Non-eruptive events may also result in degassing plumes and debris flows, but typically less meltwater which results in flows with higher concentrations of heavy metals and acids (Schaefer *et al.*, 2012). At 61^{o}N, many of the mountains are covered with a persistent mantle of glacial ice and snow, which makes any thermal event a potential for flood hazards and debris flows.

Understanding volcanic unrest events that do not lead to eruption could provide a means of predicting debris flows and degassing events associated with thermal perturbations and ice melting. Monitoring, data collection, and recording of such events, is crucial to the refinement of ice melt models and eruption prediction. This is particularly important along the Aleutian Arc because its location along a great circle route between the 48 contiguous United States and Asia makes Anchorage, Alaska the third busiest air cargo port in the world. An eruptive event could be detrimental to the safety of passenger aircraft as well as to the potential loss of cargo. Application of this model could be applied to other volcanoes, which may assist in the prediction of volcanic unrest or eruption and guide civil evacuation decisions that would reduce the likelihood of loss of life resulting from an eruptive event or from a debris flow in the case of a non-eruptive thermal event.

1.1. Volcanic Unrest

Volcanic unrest events thatculminate in an eruption cause hazards to humans that are more noticeable, and far more interesting, than those in which volcanic unrest does not culminate in an eruption. As such, it is more than likely that those events that do not culminate in eruption are

under-reported or neglected (Moran *et al.*, 2011). A failed eruption can be further defined as an event in which a magma intrusion gets close to the surface, but does not overcome the hindering forces to reach the surface (Moran *et al.*, 2011).

From the perspective of the magmatic system, there are four possible outcomes of volcanic unrest: 1) stalling at depth, with little or no degassing; 2) stalling at shallow depths within two to three kilometers of the surface, accompanied by obvious degassing; 3) a sluggish, highly viscous lava dome extrusion; or 4) an explosive magmatic eruption (Moran *et al.*, 2011).

1.2. Scope of Study

This paper investigates a non-eruptive volcanic event at Mount Spurr Volcano, Alaska. The event likely began with a shallow seismic swarm as early as October 2002, was perpetuated by another seismic swarm in July 2004 (Power, 2004; Power *et al.*, 2004), and ended in 2006 (Coombs *et al.*, 2006) with the cessation of ice melting and the re-accumulation of snow and ice at the summit of Mount Spurr (Neal *et al.*, 2007).

The purpose of this study is to develop a quantitative analysis of this episode of volcanic unrest at Mount Spurr. The timeline of events is marked by the dates of the initial seismic swarm, ice cauldron formation, and the cessation of ice melt. These data, combined with an estimate of the volume of ice melt and rate of CO_2 degassing, provide a means to estimate the thermal energy released, rate of heat flow, and a number of subsurface geophysical parameters that control the rate of heat transfer.

Section 2 discusses the location, geology, and eruptive history of Mount Spurr. In Section 3, AVO data of the non-eruptive event at Mount Spurr in 2002-2006 is analyzed and key constraints are defined. These data provide constraints on the thermal energy and power

necessary to melt the ice cauldron and heat the resulting meltwater, the duration of the thermal perturbation front, and the maximum distance of heat transport. I then outline a conceptual model of the volcanic unrest event that forms the framework of quantitative analysis. A mechanism of advective heat transport based solely on the mass flow rate and heat output transported by CO_2 degassed as a result of cracking and enhanced CO_2 release is analyzed in Section 4. Section 5 analyzes the potential for a hydrothermal system which extends from the top surface of the magma body to the base of the ice cauldron formed near the summit of Mt. Spurr and offers calculated permeability and planform area of such a system. In Section 6, a hydrothermal system enhanced as a result of degassed volatiles is discussed. A potential state of the pre-enhanced hydrothermal system is developed, changes in conductive boundary layer thickness are modeled, permeability is calculated, and a planform area that agrees with mapped phenomena is deduced. Discussions of the results and implications of this study are found in Section 7, and the conclusionsare summarized in Section 8.

2. Mount Spurr

Mount Spurr is a 3,374 m high dominantly andesitic arc strato-volcano in Alaska (Coombs *et al.*, 2012), located approximately 125 km west of Anchorage, Alaska, Figure 1 (Coombs *et al.*, 2006). Mount Spurr is the eastern-most historically active volcano in the Aleutian Arc (Coombs *et al.*, 2006). Mount Spurr summit is approximately 2.5 km north of Crater Peak (Coombs*et al.*, 2006). Both lie within a 5.5 km diameter, mostly ice filled collapsed caldera that formed in the late Pleistocene or early Holocene, Figure 2 (Nye and Turner, 1990). Recent eruptions have occurred at the summit peak of Mount Spurr at approximately 5.2 ka (Riehle, 1985), at Crater Peak in 1953 (Juhle and Coulter, 1955) and in 1992 (Keith, 1995).

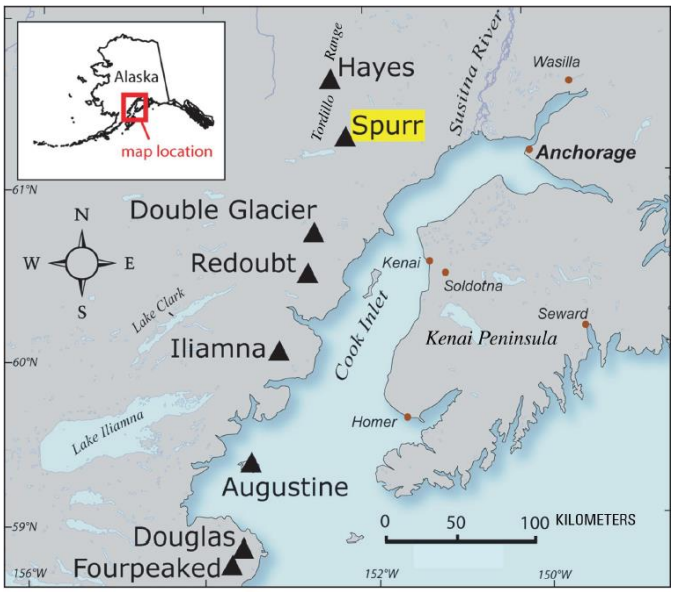

Figure 1. Cook Inlet region, southern Alaska, showing locations of Mount Spurr and other volcanoes (triangles). Dots, towns and villages. Map courtesy of Janet Schaefer, Alaska Division of Geological and Geophysical Surveys (Coombs *et al.*, 2006).

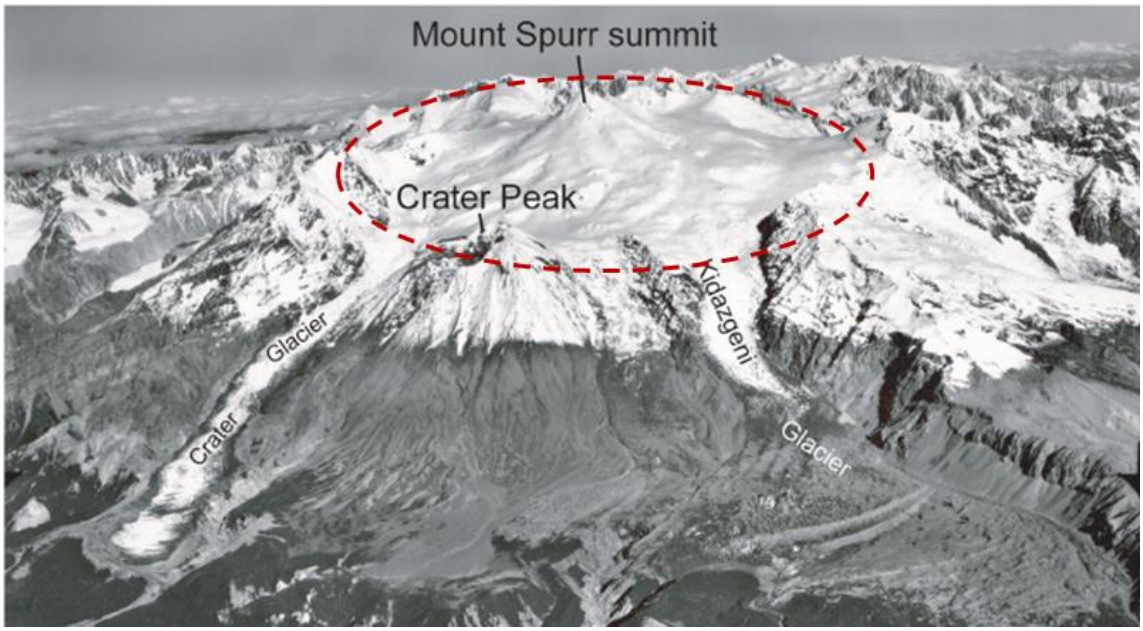

Figure 2. Spurr volcanic complex (see Figure 1 for location). Summit of Mount Spurr sits in an ice-filled collapse caldera, breached to the south; Crater Peak, a historically active satellite vent, sits in the breach. Debris-avalanche deposit in foreground, which was formed during caldera formation is dated at early Holocene (Waythomas and Nye, 2002). View northward; photograph 666-6 by Austin Post, taken September 4, 1964. Modified from (Coombs *et al.*, 2006).

3. Analysis of Key Observational Constraints and a Conceptual Model

Ice melt on summit glacier was tracked through time by using a geographic information system, digital elevation models, and aerial imagery (Coombs *et al.*, 2006). The ice mantle began to show subsidence in June 2004, resulting in the formation of an ice cauldron by 08 July 2004 (Coombs *et al.*, 2006), suggesting that heating began prior to June 2004. By August 2005, the ice cauldron was considered to have expanded to its maximum area of approximately 70,000 m^2 (Coombs *et al.*, 2006; Neal *et al.*, 2007), and depth of approximately 78 to 80 m (Coombs *et al.*, 2006). The estimated melted ice volume was approximately 5.4 x 10^6 m^3 (Coombs *et al.*, 2006). On 14 April 2006, the average temperature of the lake within the ice cauldron was 11 ^oC; see Table 1 of (Coombs *et al.*, 2006).

Table 1 provides a summarized timeline of events as recorded by the Alaska Volcano Observatory (AVO) and/or its affiliates. This summarized timeline was used to determine the timing of major events for the calculations in this portion of the study.

3.1. Minimum Thermal Energy Required to Melt the Ice and Heat the Meltwater

This section is concerned with calculating the thermal energy and heat output necessary to melt the total amount of ice melted within the cauldron, the heating of that meltwater to 11 ^oC, and the duration of the melting event. These values are considered to be minimum values, as not all of the thermal energy was captured by melting ice; the excess of which was released by fumaroles, radiant heating, or advection into the surrounding environment without measurement.

The amount of thermal energy, E, needed to melt the ice necessary to form the ice cauldron and heat the melt water is given by:

$$E = \rho i\ Vi\ [c_i\ (\ T_{fus} - T_i\ ) + L_{fus} + c_w\ (\ T_f - T_{fus})] \quad [1]$$

where ρ_i is the density of the ice; V_i, the volume of the ice melted; c_i, the heat capacity of the ice; c_w, the heat capacity of water; T_{fus}, the melting temperature of the ice; T_i, the initial temperature of the ice; L_{fus}, the latent heat of fusion of the ice; T_f, the final temperature of the meltwater. Appendix A contains symbol definitions andvalues used in calculations.

Table 1. Summary timetable of data relating to a thermal event at Mount Spurr, Alaska in 2002-2006.

Event	Date	Reference
seismic swarm, possible magma emplacement and assumed initiation of thermal event	20 Oct 2002	(Dixon *et al.*, 2003; Power, 2004; Power *et al.*, 2004)
increased seismicity	Jul 2003	(Power, 2004)
steaming rock below summit, audible gas emission, strong H_2S noted	19 Mar 2004	(Coombs *et al.*, 2006)
no deformation noted	03 May 2004	(Coombs *et al.*, 2006)
obvious subsidence in summit glacier denoting heat transfer to surface geology	20 Jun 2004	(Coombs *et al.*, 2006)
seismic swarms, possibly contributing to previous magma volume	Jul 2004	(Dixon *et al.*, 2005; Power, 2004; Power *et al.*, 2004)
obvious ice cauldron, actual date of ice plug collapse is unknown	08 Jul 2004	(Coombs *et al.*, 2006)
debris flow on the ESE flank of the summit	10 Jul 2004	(Coombs *et al.*, 2006)
effective cessation of ice cauldron growth, limited by existing geology	01 Aug 2005	(Coombs *et al.*, 2006; Neal *et al.*, 2007)
no appreciable growth in ice cauldron, meltwater temperature recorded as high as 25/45 ^{o}C, average temperature of 11 ^{o}C	14 Apr 2006	(Coombs *et al.*, 2006; Neal *et al.*, 2007)
previously steaming areas on flanks covered in snow, yellow precipitate observed along lakeshore; taken as the definitive end of this thermal event	23 Apr 2006	(Coombs *et al.*, 2006)

For simplicity, we assume that the glacial ice is initially at its melting point of 0^{o}C, soT_1 = T_{fus} = 0 ^{o}C. Equation [1], with T_2 = 11 ^{o}C and parameter values from Table 2, is then:

$$E = \rho_i\ V_i\ [\ L_{fus} + 11 c_w] \quad [2]$$

The minimum thermal energy required to melt 5.4 x 10^6 m^3 of ice and heat the resulting meltwater to 11 ^oC is approximately 2.1 x 10^{15} J; neglecting the heating of meltwater, the minimum thermal energy, *E,* becomes 1.8 x 10^{15} J, showing that a significantmajority of the heat input goes into melting the ice.

3.2. Minimum Rate of Heat Release Required to Melt the Ice and Heat the Meltwater

To calculate heat flow, it is first necessary to determine the dates of melt initiation and melt cessation. Table 2 lists the events from Table 1 which were deemed appropriate for calculating the heat flow related to cauldron growth and meltwater heating. Note that 20 Jun 2004 was selected as the date of cauldron initiation. Although steaming rock was noted on 19 Mar 2004, accompanied by audible gas emission, it was considered too early, as ice had not yet begun melting as far as observation was concerned, as per the entry on 03 May 2004 of no deformation noted. An obvious cauldron had developed by 08 Jul 2004, but was considered as too late a date, due to the fact that by the time the ice plug was able to fall in, creating the obvious cauldron, melting had been previously ongoing prior to that event. Since the thermal properties beneath the ice are unobserved, surface subsidence is the only indication of thermal energy reaching the surface, and so the date of subsidence, 20 Jun 2004 is used to delineate thermal breaching of the rock surface.

Table 2. Observed Data for Determining Heat Flow

Description	**Date**	**Reference**
obvious subsidence in summit glacier denoting heat transfer to surface geology	20 Jun 2004	(Coombs*et al.*, 2006)
effective cessation of ice cauldron growth, limited by existing geology	01 Aug 2005	(Coombs *et al.*, 2006; Neal *et al.*, 2007)
no appreciable growth in ice cauldron, meltwater average temperature recorded as 11 ^oC	14 Apr 2006	(Coombs *et al.*, 2006; Neal *et al.*, 2007)

The 21 month duration of the cauldron forming and meltwater heating event is calculated as the difference between the date of cauldron initiation, 20 Jun 2004 (Coombs *et al.*, 2006), and the date which the meltwater temperature was recorded at 11 ^{o}C, 14Apr 2006 (Coombs *et al.*, 2006); which is approximately 5.5 x 10^7 s.

From the minimum thermal energy of 2.1 x 10^{15} J calculated in Equation [2], and the 5.5 x 10^7 s duration of the event, we calculated the minimum heat flow rate to be approximately 38 MW.

3.3. A Conceptual Model of Thermal Unrest

Prior to the surface-observable unrest event at Mt. Spurr, the processes within the volcanic complex were in a thermally reduced state, or at least in a state where changes were unnoticed at the surface, suggesting a quasi-steady state of thermal flux. The onset of increased fumarolic activity and the melting of ice suggest that Mt. Spurr had received an influx of thermal energy, which altered that previous state to one of increased activity.

The conceptual model of the volcanic unrest event at Mt. Spurr assumes the presence of a crystallizing subsurface magma body at some depth beneath the Mt. Spurr summit that is separated from a shallower convecting hydrothermal system by a rheological boundary termed the brittle-ductile transition, Figure 3. At temperatures greater than approximately 500 °C, rock tends to deform in a ductile manner, whereas beneath that temperature, rock behaves as a brittle medium (Fournier, 1999). As crystallization of the magma body occurs, a single phase H_2O-CO_2-NaCl magmatic fluid exsolves from the melt, migrates to the brittle-ductile transition boundary, and ponds. The accumulating magmatic fluid results in an increase in pressure beneath the brittle-ductile transition, and the rocks eventually fracture when the pressure exceeds

the tensile strength of the overlying rocks (Fournier, 1999). Emplacement of new magma at depth or a tectonic event may also lead to rupture of the brittle-ductile boundary. Once fracturing occurs, the associated pressure drop leads to phase separation to produce a dense H_2O-NaCl brine that ponds at depth, and a CO_2-rich vapor phase that migrates upward into the bottom of a hydrothermal system. The drop in pressure as a result of breaking the seal, also results in a pressure pulse that diffuses through the overlying rock (Phillips, 1991).

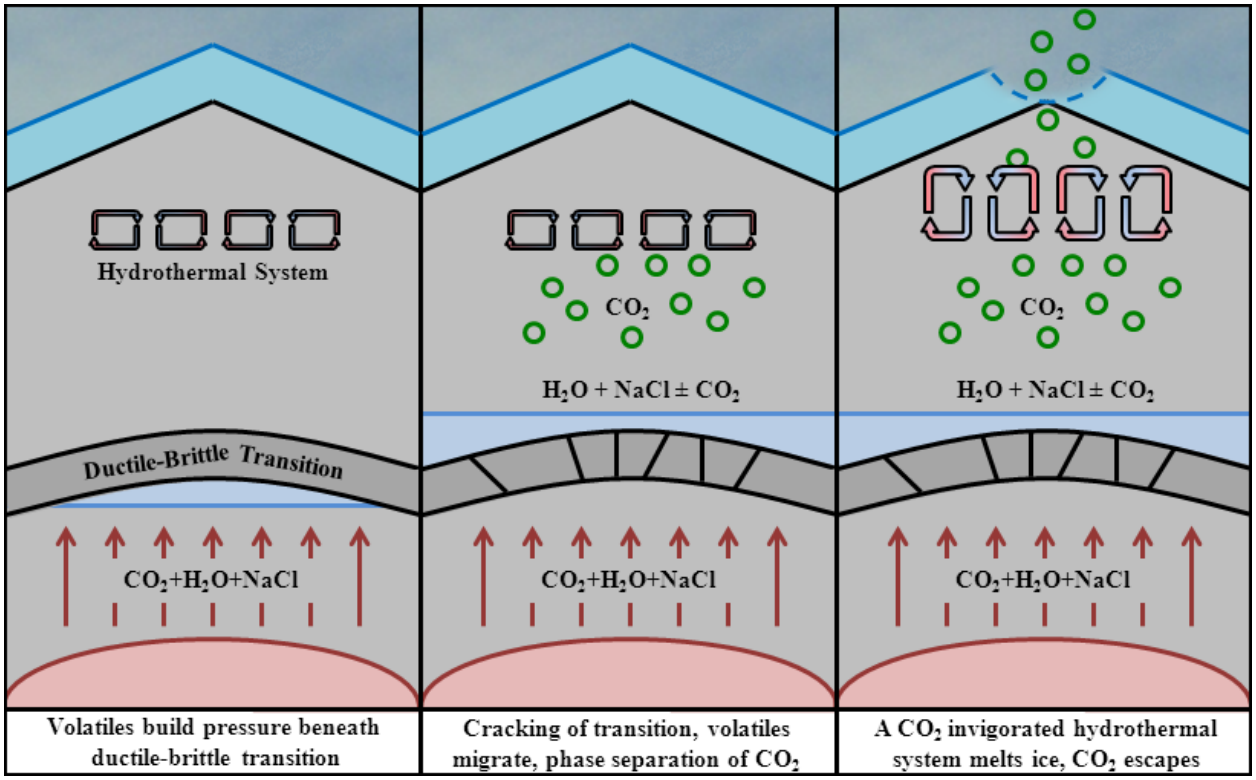

Figure 3. This figure shows the conceptual model of the Mt. Spurr system. Left: A cooling and crystallizing magma body at depth degasses volatiles, the majority of which are CO_2, H_2O, and assorted metallic chlorides. These migrate upward until they reach the mostly impermeable brittle-ductile transition and begin to collect and build pressure. Middle: Volatile pressure exceeds lithostatic pressure and ruptures the boundary, temporarily increasing permeability, and allowing the escape of the volatiles. Right: Changes in pressure from lithostatic to hydrostatic cause phase separation in the CO_2-H_2O-NaCl system allowing CO_2 gas to escape to the surface, invigorating the preexisting hydrothermal system and escaping to the atmosphere.

The hydrothermal system is assumed to extend from the brittle-ductile transition to the base of the ice sheet, though the most vigorous circulation is thought to extend only to a depth of a few kilometers (Motyka and Nye, 1993) as suggested schematically in Figure 3. The pressure pulse, together with the CO_2 phase, transfers thermal energy and mechanical energy from depth into the shallow hydrothermal system. The increased thermal energy and likely increase in rock permeability likely enhances the vigor of hydrothermal heat transfer to the base of the ice layer. Some of the CO_2 dissolves into the convecting hydrothermal fluid, but some of the CO_2 moves as a separate phase through the hydrothermal system and transfers heat to the ice layer at the Mt. Spurr summit.

The unrest event discussed in this study began with seismic activity (Coombs *et al.*, 2006; Power *et al.*, 2004), continued with increases in fumarolic activity and outgassing (Coombs *et al.*, 2006; Doukas and McGee, 2007), the melting of 5.4×10^6 m^3 of ice which caused debris flows (Coombs *et al.*, 2006), and ended with the cooling of the edifice, evidenced by the re-accumulation of snow and ice (Neal *et al.*, 2007). To investigate the mechanism of heat transport, we focus on that portion of the event which altered the thermal state of Mt. Spurr volcano; from the date of the initiating seismic swarm to the date of noticeable surface ice melt.

Figure 4 shows a bar chart of seismic activity beneath Mt. Spurr as a function of time from 1991 to July 2004. The figure shows significant increases in seismicity associated with the 1992 eruption as well as other seismic swarms in October 2002 and July 2004 (Power, 2004).

As suggested by Power (2004), I consider the seismic swarm in October 2002 to be the initiation of the unrest event, which I interpret to be a manifestation of a cracking event and release of volatiles. The seismic swarms in 2003 and 2004 may be associated with additional crustal cracking associated with magma degassing. The timeframe of the thermal perturbation

front is then the second fundamental constraint, beginning in Oct 2002 and affecting the surface by Jun 2004, a duration of 20 months, approximately 5.3 x 10^7 s.

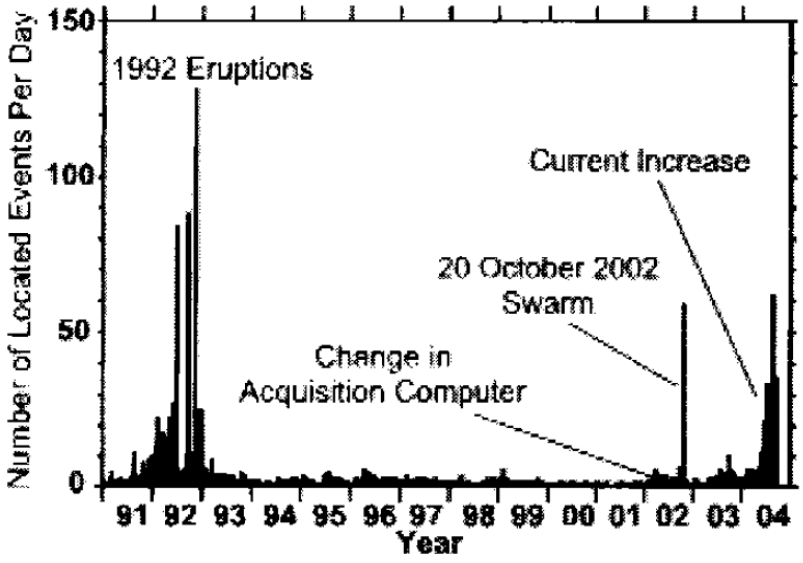

Figure 4. Shows the number of earthquakes within 20 km of Mount Spurr from 1991 to mid-2004. Note the small increase in earthquake activity in mid to late-2003 which predates the earthquake swarm in 2004 and the small increase in earthquake activity in early 2001, attributed to changing to the Earthworm acquisition system, which predates the 2002 swarm. A similar character can be found in early to mid-1991, predating the 1992 eruption. from (Power, 2004).

3.4. Maximum Distance of Heat Transport

In this section, I discuss the maximum distance that heat must travel through the volcanic edifice. It is this measure which will assist in determining the mechanism of heat transfer. This maximum depth is determined by the seismicity recorded at Mt. Spurr during the events as shown in Figure 5.

Figure 5 shows that the 2002 and 2004 hypocenters are generally located beneath the summit of Mt Spurr; their distribution suggests a concentration of hypocenters at a depth of approximately 5 km. Review of the seismic velocity model (Jolly *et al.*, 1994) indicates that

there is a concentration of seismic activity at the depth of 8.4 km beneath Mt. Spurr summit, associated with the shoaling of the brittle-ductile transition to a depth of 5 km below sea level directly beneath the volcanoes of the Cook Inlet. Along the Cook Inlet volcanic axis, however, an uncertainty of ± 2.8 km is associated with the 2002 and 2004 seismic swarm data (Dixon *et al.*, 2005; Dixon *et al.*, 2003) suggesting that the actual distribution of hypocenters may be spread between 5.6 km and 11.2 km depth beneath the Mt. Spurr summit.

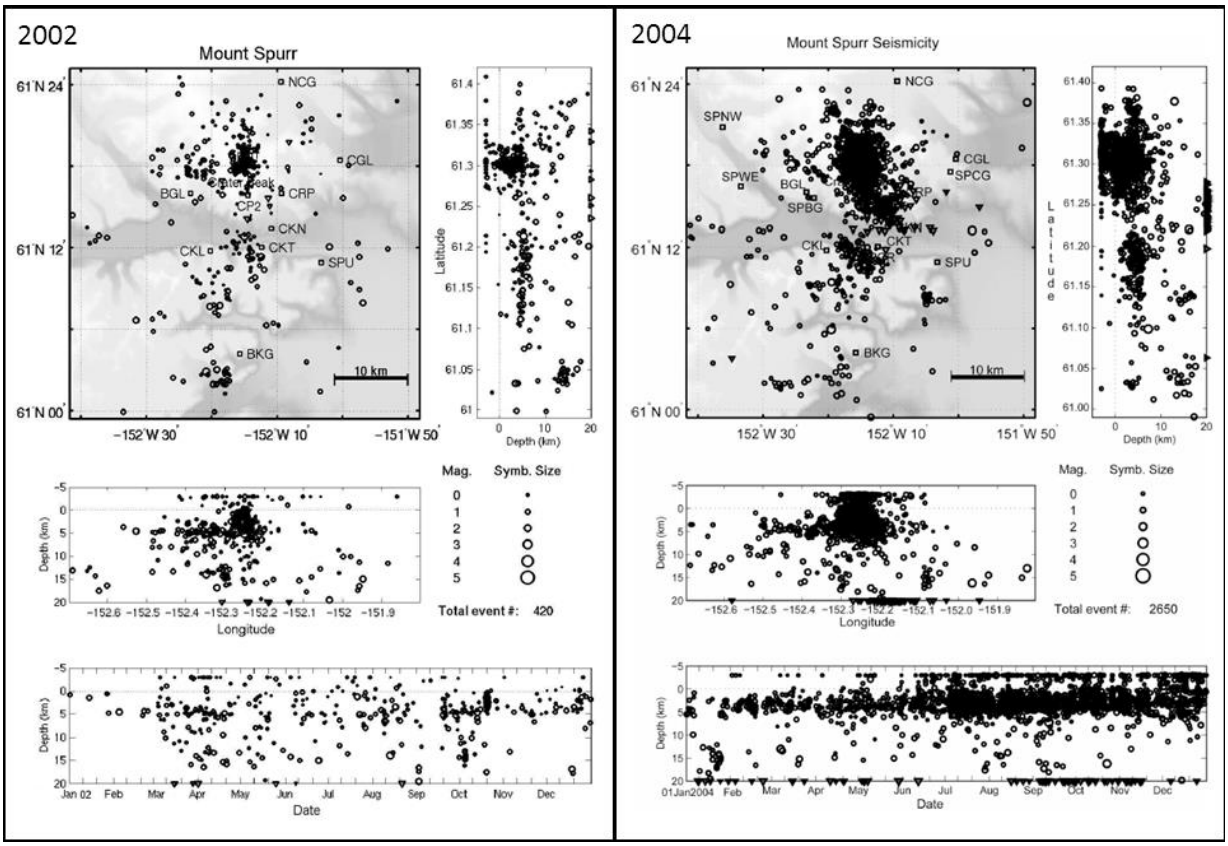

Figure 5. (left) A plot of the seismicity of 2002, including the seismic swarm of 20 October 2002, showing a trend at an approximate depth of 5 km. from Figure A2 of (Dixon *et al.*, 2003). (right) A plot of the seismicity of 2004, including the increased seismicity of July 2004 and onwards. from Figure A2 of (Dixon *et al.*, 2005).

Assuming that 5 km depth below sea level represents the brittle-ductile transition (Jolly *et al.*, 1994) and the summit of Mount Spurr is approximately 3,374 m high (Coombs *et al.*, 2006), the

maximum distance heat must travel is then approximately 8 km. Using the maximum distance, and the duration of 5.3 x 10^7 s calculated in the previous section, the maximum velocity of heat transfer is approximately 1.5 x 10^{-4} m/s.

3.5. Potential Mechanisms for Heat Transport

There are three possible mechanisms for heat transport within Mt. Spurr volcano: 1) magmatic degassing of volatiles associated with the observed increase in CO_2 flux between 2004 and 2006 (Doukas and McGee, 2007), 2) hydrothermal convection from the brittle-ductile transition to the volcanic surface of the summit of Mt. Spurr, near the base of the ice, and, 3) a combination of the enhanced CO_2 flux coupled with enhanced hydrothermal activity beneath the summit that results from the increased CO_2 flux between 2002 and 2004. The next three sections cover these mechanisms in more detail.

4. Melting Ice and Heating Meltwater via Magmatic Degassing of Volatiles

This section begins by determining an amount of CO_2 necessary to melt the ice and heat the meltwater to 11 ^oC and comparing that to the observed emissions data. Furthermore, it explores the possibility of enhanced hydrothermal heat transfer resulting from an increase in CO_2 emissions.

4.1. Minimum Mass and Mass Flux of CO2 Derived from Cauldron Formation and Lake Heating

In this section we determine the minimum mass and resulting mass flux of CO_2 necessary to melt the 5.4 x 10^6 m^3 of ice and to heat the resulting meltwater to 11 ^oC. This is a minimum due to the assumption that all the available heat from degassed CO_2 went into melting the ice and

heating the meltwater to 11 ^{o}C, with no regard for heating the edifice on its rise to the surface. Forward Looking Infrared images (FLIR), taken by AVO, of the episodic debris flows sourced from the meltwater lake indicate a decrease in temperature from the debris flows in June and July 2004, to those in May 2005 (Coombs *et al.*, 2006). This suggests that the temperature of the meltwater may have been higher than the lake average of 11 ^{o}C that was recorded on 14 Apr 2006.

From Equation [2], the minimum thermal energy required to melt the 5.4 x 10^6 m^3 of ice and to raise its temperature to 11 ^{o}C, was calculated to be 2.1x 10^{15} J. The minimum mass of CO_2 necessary to obtain this amount of thermal energy can be solved for by using an energy balance equation. By rearranging the equation $E = m\ c\ T$ and substituting the calculated thermal energy for E, the mass of CO_2 can then be solved for by:

$$m = E / (c_{CO2}\ T) \qquad [3]$$

where m is the mass of CO_2, c_{CO2} the specific heat capacity of CO_2, and T is the temperature. Figure 6 shows how the mass of CO_2 necessary changes with the temperature of that CO_2 from 200 °C, which corresponds to the approximate hydrothermal temperature (Garchar *et al.*, 2012), and 1000 °C, which corresponds to the approximate temperature of andesitic magma. CO_2 released at the brittle-ductile transition would have a temperature of approximately 500 °C (Fournier, 1999).

The minimum necessary mass of CO_2 at 1000 ^{o}C to melt the ice and heat the meltwater is found to be approximately 1.7 x 10^9 kg, approximately 1.7 x 10^6 tonnes; CO_2 at a temperature of 200 ^{o}C would take approximately 8.3 x 10^9 kg, or 8.3 x 10^6 tonnes; at 500 ^{o}C, 3.6 x 10^9 kg. Whereas the melting event lasted 5.5 x 10^7 s, we further determine the minimum mass flux of

CO_2 at 1000 ^oC to be 31 kg/s, or 2.7 x 10^3 t/d; CO_2 at 200 ^oC would require 150 kg/s, or 1.3 x 10^4 t/d; at 500 ^oC, 66 kg/s or 5.7 x 10^4 t/d.

These mass fluxes, Q, can alternatively be determined by:

$$Q = H / c_{CO2}\, T \qquad [4]$$

where H is the heat output determined in Section 3.2, c_{CO2} is the heat capacity of CO_2, and T is the temperature.

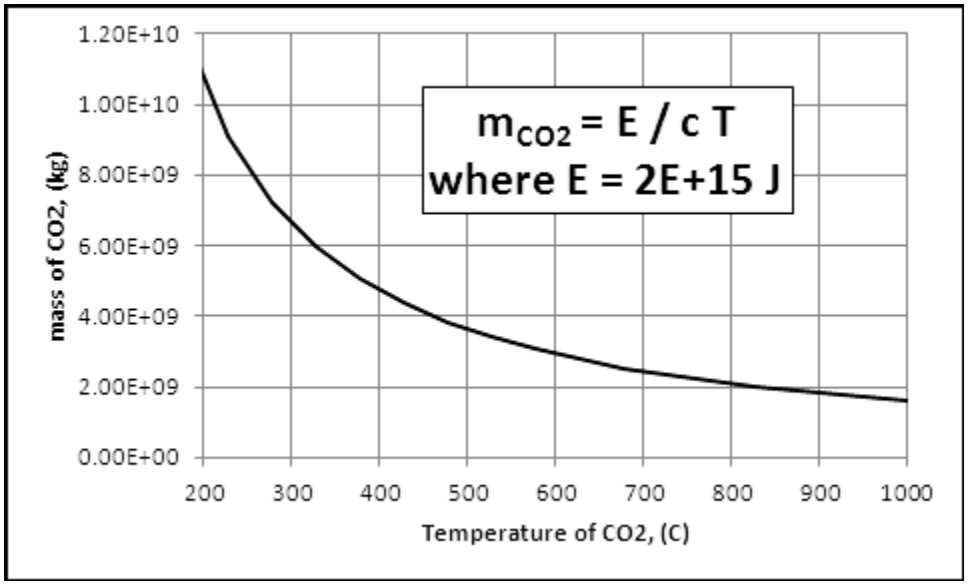

Figure 6. Shows the relationship between the temperature of a mass of CO_2 and the amount of mass of CO_2 needed to produce 2x10^{15} J of thermal energy, using an expression for the specific heat of CO_2 as a function of temperature (Lemmon *et al.*, 2011).

4.2. Heat Output of CO_2 Derived from Observed Emissions

Prior to the presumed cracking event evidenced by the increased seismicity in Oct 2002, Figure 4, background degassing may be attributed to a residual magma body. The cracking event would then increase the volatile emissions, as suggested in Figure 3.

Volatile emission from Mount Spurr was evidenced on 19 March 2004 by climbers in the area of the as of yet unformed ice cauldron, they stated the presence of steaming rocks below the summit as well as a strong odor of H_2S, which was later confirmed on 11 July 2004 by a local Alaskan pilot noting a steam plume at ~1650 m and the odor of SO_2 (Coombs *et al.*, 2006).

Since its eruption in 1992, degassing of both SO_2 and CO_2 have continued at background levels ranging from a few tonnes per day of SO_2 and under 200 tonnes per day of CO_2 (Coombs *et al.*, 2006). Observed emissions during the non-eruptive event in this study were monitored at irregular intervals from 08 August 2004 (Doukas and McGee, 2007; Werner *et al.*, 2011) when emission levels significantly increased beyond background emissions, until they again subsided in November 2006. Tabulated results from (Doukas and McGee, 2007) were graphed by (Werner *et al.*, 2011) and are shown in Figure 7.

Date	SO_2 rate t/d	CO_2 rate* t/d
SPURR SUMMIT		
08/07/04	0	609
09/15/04	0	1300
09/16/04	0	1167
10/29/04	0	1400
02/28/05	83	327
03/02/05	47	536
05/10/05	110	750
05/11/05	72	760
09/20/05	54	246
04/06/06	184	–
04/23/06	62	184
04/26/06	49	498
07/12/06	100	–
08/28/06	53	–
09/25/06	64	150
11/17/06	390	308

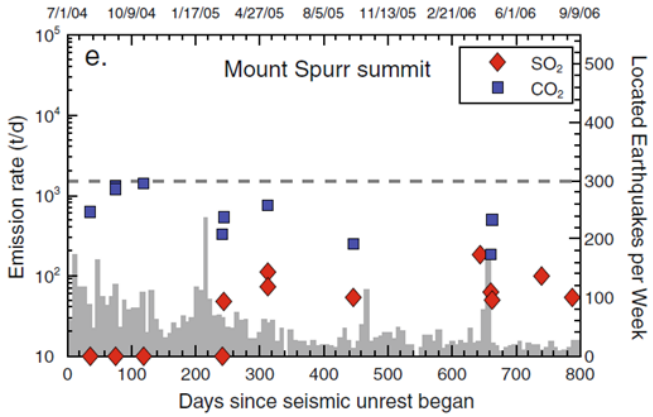

Figure 7. An excerpt from Table 1 of (Werner *et al.*, 2011) showing the observed degassing rates of CO_2 and SO_2 from Mount Spurr between the dates of 7 August 2004 and 17 November 2006 and the associated graph of that data. From the initial date of monitoring to 16 Apr 2006, the date of the AVO FLIR measurement noting the meltwater lake temperature at an average of 11 ^{o}C, the average CO_2 emissions were788 t/d. modified from (Werner *et al.*, 2011).

The following calculations are conservative as they include the assumptions that: (1) the observed CO_2 consisted of the total degassed CO_2, which is unlikely, and (2) all of the thermal energy from the CO_2 is 100% efficient in rising from the magma intrusion to the base of the ice with no pathway losses of thermal energy. Some of the losses incurred are due to the initial emissions of CO_2 transferring some of its thermal energy to the surrounding rock and hydrothermal fluid, further supporting that CO_2 degassing could not have been the sole mechanism of heat transport to the surface, or that CO_2 degassing was initially much higher than that recorded later in the sequence of volcanic unrest.

The average of the observed mass flow rate, Q, of CO_2 from 07 Aug 2004 to 14 Apr 2006 is calculated to be 788 tonnes per day, approximately 9 kg/s. Heat output, H, of the CO_2 emissions can be calculatedby:

$$H = c_{CO2}\, Q\, T \qquad [5]$$

where c_{CO2} is the specific heat capacity of CO_2, and T corresponds to an assumed magmatic temperature of 500 ^{o}C. The resulting heat output of approximately 5 MW, is about 14% of the 38 MW necessary to form the ice cauldron and increase the meltwater temperature to 11 ^{o}C during its 21 month duration. Using a CO_2 temperature of 200 ^{o}C would result in a thermal output of approximately 2.2 MW, approximately 6% of that needed.

Scaling backward, if this same mass flux at 500 ^{o}C had begun a year earlier, effectively doubling the heat output, it would still only provide 10% of that necessary to melt the ice cauldron and heat the meltwater to 11 ^{o}C. It is only if we assume that these same emissions began in July 1990, which predates the previous eruption of 1992, that the heat output by CO_2 could account for all that is required. This result suggests that initially, CO_2 output must have

been greater than that observed between 2004 and 2006. It is also likely that the initial CO_2 output did not melt the ice directly, but rather warmed the underlying rock and hydrothermal fluid leading to enhanced hydrothermal heat output. Using the maximum recorded value of 1400 t/d on 29 Oct 2004 results in a value that is 25% for CO_2 at 500 ^oC, 11 % at 200 ^oC. This analysis suggests that CO_2 emissions cannot be the sole mechanism of heat transfer if degassing coincided with a seismic swarm around August 2004.

5. Characterization of a CO_2 Enhanced Hydrothermal System

It has been shown in the previous section that degassed CO_2 alone is most probably not the sole provider of thermal energy to the surface of Mount Spurr.

Rather than assume that hydrothermal fluid must move from the top of the newly emplaced magma to the base of the forming ice cauldron, I assume that the base of the hydrothermal system lies much higher in the volcanic edifice. Using controlled-source audio-magnetotelluric, self-potential, and Hg and He soil-gas surveys from Turner and Wescott (1986), Motyka and Nye (1993) constructed a conceptual model of a hydrothermal system beneath Crater Peak, at a depth ranging between 2000 and 2500 m below the summit, and as shallow as 1000 m below the surface along the flank, Figure 8. Power *et al.* (1998) suggests that the hydrothermal system may extend to 4000 m beneath the summit, but here we use the more conservative value of 2000 m. Such a hydrothermal system may not be directly connected to a magmatic heat source at depth. Rather, a preexisting hydrothermal system may be rejuvenated by enhanced volatile flux stemming from a cracking event above a cooling magma at some unknown depth beneath the volcano or from the emplacement and cooling of a newly emplaced batch of magma (Motyka and Nye, 1993).

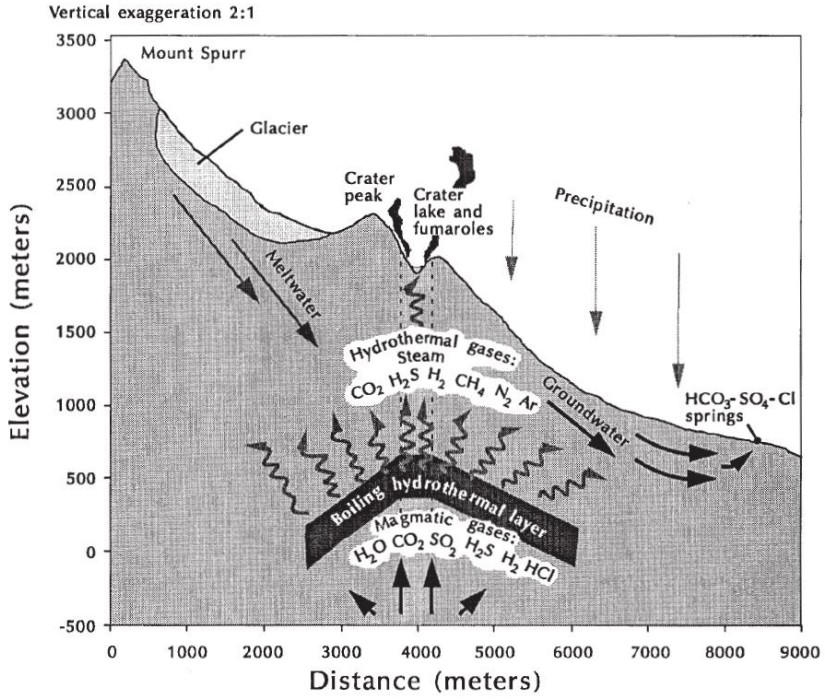

Figure 8. "Conceptual model of the Crater Peak hydrothermal system. Residual 1953 magma at unknown depth expels steam, CO_2, SO_2, HCl and other magmatic gases into overlying hydrothermal layer that was formed by post-1953 infiltration and accumulation of ground water. Steam and gases rich in CO_2 and H_2S are driven off the boiling hydrothermal layer and feed fumaroles at Crater Peak summit crater and interact with shallow groundwaters to produce HCO_3–SO_4–Cl thermal springs at lower elevations." from Figure 4 of (Motyka and Nye, 1993)

In this case, volatile release resulting from a cracking eventat the brittle-ductile transition may enhance hydrothermal heat outputbeneath the ice cover.

In this section we show how a CO_2-enhanced hydrothermal system, circulating higher up in the volcanic edifice, could provide additional thermal energy to the ice at the summit of Mount Spurr.

5.1. Modeling the Conductive Layer

Consider a hydrothermal system existing in a quasi-steady state that was then perturbed by the degassing of volatiles from below (Power *et al.*, 2004), see Figure 9.

Prior to the addition of heat by newly released volatiles, hydrothermal heat was transferred across a conductive layer, δ, such that hydrothermal heat transfer did not result in melting ice on the surface. As a result of increased CO_2 flux from below, the newly invigorated system then provides more heat, thus diminishing the conductive layer allowing for a more rapid transport of heat into the ice. Alternatively, increased CO_2 output may lead to fracturing and increased permeability of the hydrothermal system. The minimum, initial conductive layer thickness, δ_i, is then shown to be equal to the ratio of the final Rayleigh number, Ra_f, to the initial Rayleigh number, Ra_i, multiplied by the final thickness of the conductive layer, δ_f:

$$\delta_i = \delta_f \frac{Ra_f}{Ra_i} \qquad [6]$$

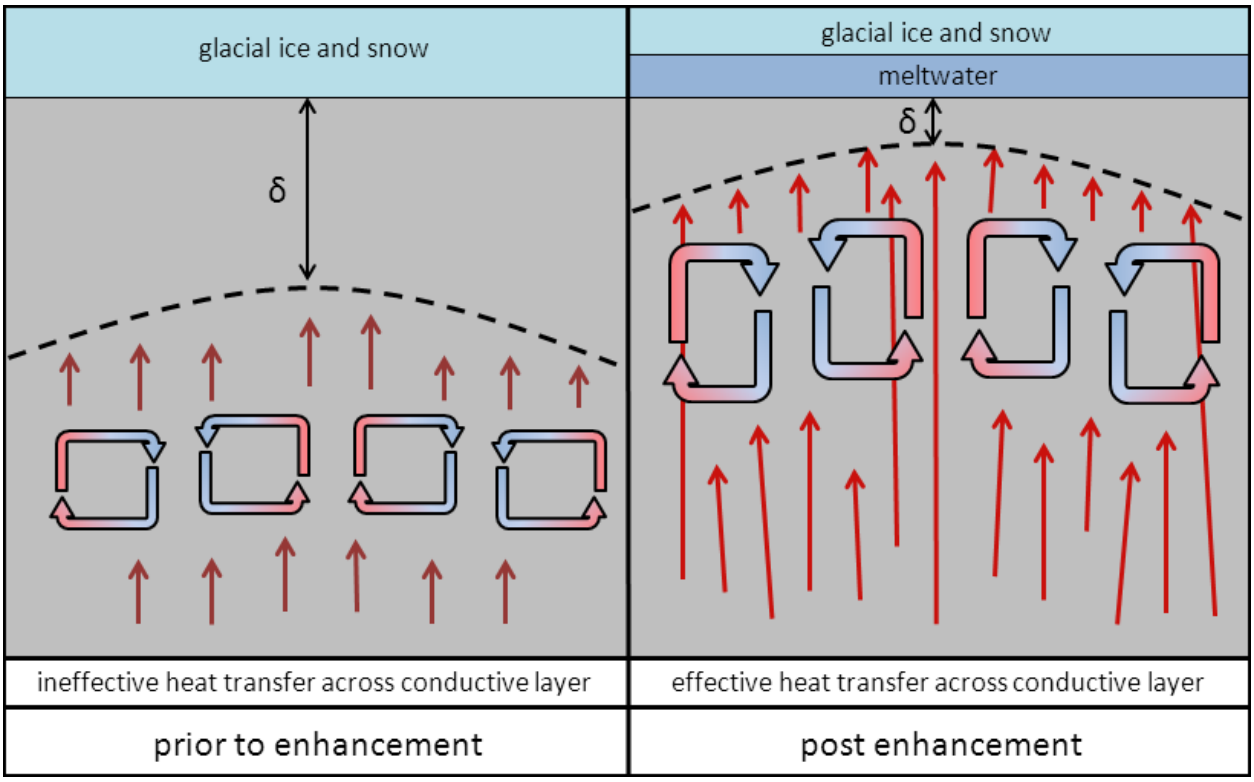

Figure 9. Left, the conductive layer δ is sufficiently thick enough so as heat cannot effectively be conducted across the boundary. Right, increased heat input from below has invigorated the hydrothermal system, increasing its convective vigor and thus its characteristic Rayleigh number, such that the conductive layer has been sufficiently decreased so as to allow effective conductive heat transport.

Furthermore, it can be shown (see Appendix B) that for an increase in Rayleigh number, the final conductive layer thickness is related to an increase in Rayleigh number by the equation:

$$\delta_f = \sqrt{\frac{a^* t}{\left[\frac{Ra_f}{Ra_i} - 1\right]}} \qquad [7]$$

where a^* is the effective thermal diffusivity of the system, and t is the 5.3 x 10^7 s duration from the start of the thermal impulse to the time that impulse reaches the surface, calculated in Section 3.3. The underlying assumption in deriving Equation [7] is that the time, t, is the time needed to move the boundary layer from its initial to its final state.

Figure 10 shows that conductive layers with Rayleigh number ratios less than 1.5, the values of δ_i and δ_f are virtually indistinguishable, consequently we consider cases for Rayleigh number ratios between 2 and 10.

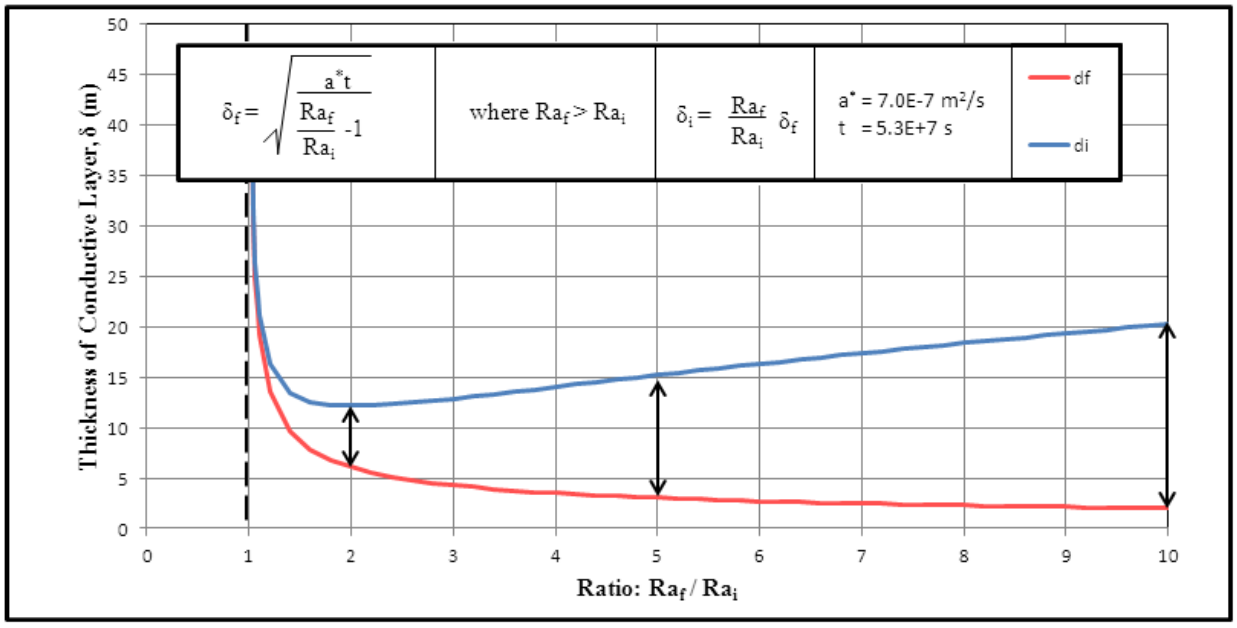

Figure 10. A plot of the initial conductive layer minimum and the final conductive layer maximum with respect to the ratio of an invigorated system's higher final Rayleigh number to that system's less invigorated initial Rayleigh number.

Assuming that the initial Rayleigh number is associated with a hydrothermal fluid of approximately 200 ^{o}C (Garchar *et al.*, 2012; Motyka and Nye, 1993) an increase in *Ra* could be associated with an increase in hydrothermal temperature associated with enhanced CO_2 release. Because both thermal expansion coefficient and viscosity are strong functions of temperature, only a modest increase in hydrothermal temperature would result in doubling *Ra.* Mechanical fracture of the edifice could also significantly and increase permeability (Bredehoeft and Ingebritsen, 1990). The constraining factors of Equation [6] are the effective diffusivity, which does not vary significantly over the temperature range of the hydrothermal system, and the duration of the thermal state change, *t*, from increased subsurface heating to surface melt.

Given the 5.3 x 10^7 s duration of the thermal impulse event, *t*, calculated from Section 3.3, and by the effective thermal diffusivity, a^*, the final thickness of the conductive layer, δ_f, of a doubled Rayleigh number would then be approximately 6 m and the initial thickness of the conductive layer 12 m. Increasing the temperature to 400 °C, for example, would also lead to an increase in α and a decrease in ν, resulting in an increase in *Ra* of at least a factor of five. This would result in δ_f = 3 m and δ_i = 15 m, respectively. The additional release of CO_2 could also lead to cracking and enhanced permeability of the hydrothermal system (Bredehoeft and Ingebritsen, 1990; Ingebritsen and Manning, 2010; Koulakov *et al.*, 2013). A tenfold increase in Rayleigh number results in δ_f = 2 m and δ_i = 20 m.

The planform area, *A*, of the hydrothermal system can be approximated by:

$$A = \frac{H\,\delta}{\lambda\,\Delta T} \qquad [8]$$

where *H* is the 38 MW minimum heat output of the ice melt and meltwater heating event; δ, the thickness of the final conductive boundary layer; λ, the thermal conductivity of andesite; and ΔT, the temperature difference between the top and bottom of the hydrothermal system, which yields

a minimum area of approximately 4 x 10^5 m^2. By using the relationship of an area of a circle to that circle's radius, we obtain a radius of approximately 357 m. Neal *et al.* (2007) estimate the radius to be 300 m, which is in good agreement with this result.

One can also estimate the radius of the surface expression of the hydrothermal system by investigating the area of fumarolic activity from the GIS map of Mt. Spurr (Coombs *et al.*, 2006) shown in Figure 11. By finding the centroid of the fumarolic activity, a best fit circle can then be estimated and a radius measured, which in this instance is approximately 410 m, an area of 5.3 x 10^5 m^2, a 14% difference in radius resulting in a 28% difference in area with that area calculated in Equation [8].

5.2. Permeability of the Volcanic Edifice

In a vigorously convecting hydrothermal system, the relationship between the thickness of the conductive boundary layer, δ, velocity of fluid transport, u, and the effective thermal diffusivity, a^*, can be scaled by the relationship (Bejan, 1995):

$$\delta = \frac{a^*}{u} \qquad [9]$$

Permeability, k, can be calculated by solving Equation [9] for velocity, u, substituting into Equation [13], then rearranging to solve for k:

$$k = \frac{\nu a^*}{\alpha g \Delta T \delta} \qquad [10]$$

where ν is the kinematic viscosity of the fluid; a^* is the effective thermal diffusivity where $a^* = \lambda / (\rho_w c_w)$, λ is the thermal conductivity of andesite, ρ_w is the density of water, and c_w is the heat capacity of water; α is the thermal expansion coefficient of the hydrothermal fluid; g is acceleration due to gravity; k is the permeability; ΔT is the change in temperature of the hydrothermal system of 200 ^oC; and δ_i is the initial thickness of the conductive layer of 12 m as

calculated in Equation [7]. The mean permeability is shown to be approximately ~10^{-14}, which is more expected and more acceptably within the range of ~10^{-11} to ~10^{-15} m^2 for fractured igneous rock (Freeze and Cherry, 1979).

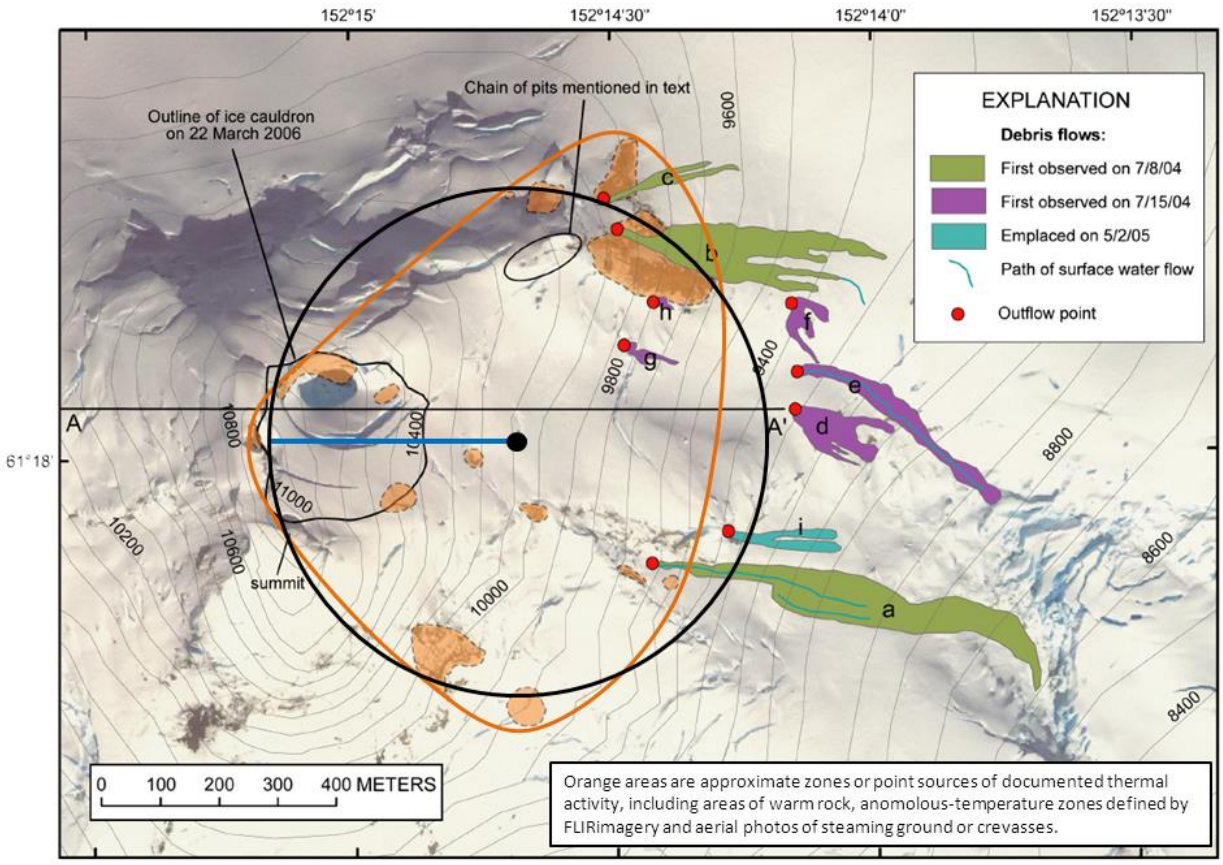

Figure 11. The orange outline roughly delineates the area of fumarolic activity, and potentially the area of the hydrothermal system's planform surface expression. The black dot marks the centroid of the irregular planform expression, and the black circle an estimated circle of equal area to the irregularly shaped planform area. The blue line marks the radius of that circle. Modified from (Coombs *et al.*, 2006) .

5.3. Additional Investigation of CO_2 Release

As a magma body cools, CO_2 and other volatiles are degassed and travel upward through the permeable medium, transferring heat to the rock and hydrothermal fluids. If the hydrothermal

fluid is under-saturated, the volatiles will dissolve into the fluid and reach thermal equilibrium with the rock and fluid surroundings. Once saturation occurs, a continuing flux of volatiles will pass through the circulating hydrothermal fluid, transfer some heat to the fluid and adjacent rock, and escape to the surface. One effect of the volatile transfer is to heat the hydrothermal system, resulting in an increased Rayleigh number and a thinning of the conductive boundary layer as described in Section 5.1. Here, I estimate the amount of CO_2 needed to heat the hydrothermal system and adjacent rock within the Mt. Spurr volcanic edifice.

The heat energy, E, contained within a mass, m, of CO_2 at an assumed magmatic temperature T_m, = 1000 ^oC, can be found by a rearrangement of Equation [3]:

$$E = m\, c_{co2}\, T_m \qquad [11]$$

where c_{co2} is the heat capacity of CO_2 appropriate for the temperature. The mass, m, needed to raise the temperature of the rock and fluid in the hydrothermal system by an amount ΔT is then given by:

$$m = V\, \Delta T\, [\, \varphi\, \rho_w\, c_w + (1-\varphi)\, \rho_a\, c_a\,] \,/\, c_{co2}\, T_m \qquad [12]$$

where V is the volume to be heated and φ is the porosity. This expression assumes that the hydrothermal fluid remains in the liquid phase, and that the CO_2 flux does not heat the rock beneath the hydrothermal system. Assuming a constant porosity of 0.10 and a cylindrical volume 2000 m high and a basal area of 4 x 10^5 m^2 as calculated in Equation [8] and ΔT = 100 °C, the minimum required mass m of CO_2 is 2.5x 10^{11} kg is required to heat the hydrothermal system as described to deliver 1.2 x 10^{18} J of thermal energy.

6. Discussion

6.1. Uncertainties in the Analysis

In this paper, I have used a variety of data sets associated with the non-eruptive volcanic event at Mt. Spurr Alaska between 2002 and 2006 to assess the roles of CO_2 flux and enhanced hydrothermal activity as mechanisms for driving the observed formation of the ice cauldron and heating of the melt water. Although the data provide a detailed timeline of events beginning with increased seismic activity in 2002 and culminating with the cessation of the event in 2006, a number of uncertainties prohibit a unique assessment of the driving mechanisms.

The first of these uncertainties would be that we assume the ice melted and heated the lake to only 11 ^{o}C, but it may have been greater, and then cooled to 11 ^{o}C. Once the cauldron had been formed, there was continued fumarolic activity and likely heating of the surrounding rock, this potential additional heat lost to the environment was not accounted for. Hence the amount of heat needed to describe the thermal event, whether by volatiles alone or by a combination of volatile release and hydrothermal activity is somewhat uncertain. Geochemical arguments suggest that the base of the hydrothermal system may have begun at 200 ^{o}C, but the final temperature of the system is an unknown, and therefore the amount of increased heat to be provided by CO_2 is also an unknown. It is not fully clear as to whether the outflow of the debris flows exactly matches the volume lost in lake level, possibly there was sub-glacial ice melted as meltwater transferred heat to the underside of glaciers as it traveled downhill.

There is little constraint on the physical dimensions and makeup of the hydrothermal system. The actual thickness, depth, and planform area of the hydrothermal system is not measurably quantified and the chemical composition of the hydrothermal fluid is unknown. As stated

previously, there is no direct temperature data for the hydrothermal system. It is these factors we use to determine such values as Rayleigh number and permeability. However, the calculations seem reasonable within the constraints of the available data.

Although there has been a suggested range of permeability for a volcanic regime, there is no actual quantifying data to suggest the actual permeability within the edifice of Mt. Spurr. Permeability exerts the primary control on convective vigor, and it seems likely that changes in permeability resulting from pressurized volatiles enhanced the permeability of the pre-existing hydrothermal system.

As a result of these uncertainties, I used lower estimates for the amount of thermal energy released in the event and this lower estimate is used to estimate both the required CO_2 flux and the hydrothermal vigor. Despite these uncertainties, however, I think a number of important conclusions can be reached concerning this event.

6.2. Implications of the Results

Despite the uncertainties the in analyses performed here, one can make inferences regarding the potential for predicting magmatic unrest events at Mt. Spurr. Based on the conceptual model used here, the occurrence of an unrest event is linked to exsolution of magmatic volatiles that pond beneath the brittle-ductile transition and advectively transport thermal and mechanical energy to the surface when that impermeable barrier is broken. If one knew the composition of the magmatic fluids, the strength of the brittle-ductile transition, and the mechanisms that lead to rupture, a time frame could be determined as to the potential for subsequent events of unrest. Such data are not available for Mt. Spurr, and may be difficult to know in advance at any volcano; however, increased seismicity concentrated at a depth near the brittle-ductile transition

likely signal breach of that impermeable barrier and the initiation of a volcanic event. For the unrest event at Mt. Spurr between 2002 and 2006, there was a period of more than a year between the initiation of seismicity in October 2002 and the surface expression of ice melt and CO_2 flux to the atmosphere that began in June/July 2004. The delay time between rupture of the brittle-ductile transition and release of volatiles most likely corresponds to (a) the time for the pressure perturbation to propagate from the brittle-ductile transition to the base of the hydrothermal system, and (b) the time for CO_2 to migrate through the volcanic edifice to the surface. The time scale τ_p for diffusion of the pressure pulse that occurs as a result of breaking the brittle ductile seal and changing the pressure from lithostatic to hydrostatic can be estimated from the expression:

$$\tau_p \sim L^2/a_p \qquad [13]$$

where L is the approximate 6 x 10^3 m distance between the brittle ductile transition and the base of the hydrothermal system and $a_p = k\, c_1^2 / v\phi$ is the coefficient of pressure diffusivity (Phillips, 1991). In this expression, k is the permeability of ~10^{-14} as calculated in Equation [10], $c_1 \sim 1.4$ x 10^3 m/s is the speed of sound in water, v is the kinematic viscosity of the fluid as defined in Appendix A, and φ is the assumed 0.1 porosity of the host medium. The pressure diffusivity is then ~ 0.65 m^2/s, which yields a pressure diffusion time scale of ~ 5.5 x 10^7 s, for a travel distance of 6 km. The permeability at depth is likely less than that estimated for the hydrothermal system in the upper part Mt. Spurr; however, this would be offset by a decrease in porosity as well as a decrease in fluid viscosity that would accompany an increase in temperature at depth.

The pressure pulse along with CO_2 transport at a temperature of approximately 500 °C, the approximate temperature of the brittle-ductile transition, likely contribute together to enhancing

the Rayleigh number, and hence heat transport, of the hydrothermal system circulating within the volcanic edifice. It appears from our calculations that it is enhanced heat transport from the hydrothermal system that is mainly responsible for the ice melting event at Mt. Spurr summit rather than directed heating by the observed CO_2 flux. Hence understanding the time delay between cracking the permeability seal that can be seen from seismicity data and the response of the hydrothermal system to this event can assist in planning for evacuation and/or diversion of people and cargo from the area.

7. Conclusions

The results of the analyses presented here indicate that the observed amount of CO_2 flux cannot provide the heat necessary to form the ice cauldron and heat the resulting meltwater, therefore, CO_2 emission cannot be the sole mechanism of heat transport.

A pre-existing hydrothermal system enhanced by CO_2 emission does have the capability to transport the required amount of heat in the required amount of time, provided that CO_2 can increase the Rayleigh number of the hydrothermal system by a factor of ten. This invigoration more likely results from increased permeability caused by the episodic release of pressurized CO_2 than by an increase in ΔT across the hydrothermal system. Based on the heat needed from hydrothermal activity, the permeability in the upper 2 kilometers of Mt Spurr is ~ 10^{-14} m^2.

The increase in seismic activity leading up to and including the event of unrest is more likely caused by pressurized volatiles cracking less permeable strata and making their escape, leading to an increase of observed volatile flux and subsequent heating, rather than the emplacement of a new magma body.

Bibliography

Bejan, A., 1995. Convection Heat Transfer. John Wiley & Sons, New York, 623 pp.

Bredehoeft, J.D. and Ingebritsen, S.E., 1990. Degassing of carbon dioxide as a possible source of high pore pressures in the crust. The Role of Fluids in Crustal Processes: 158-164.

Coombs, M., Calvert, A., Vallance, J. and Sisson, T., 2012. Pleistocene-present growth and erosion of ice-covered Spurr volcanic complex, Alaska, Volcano-Ice Interactions on Earth and Other Planets Conference III, Anchorage, Alaska.

Coombs, M.L., Neal, C.A., Wessels, R.L. and McGimsey, R.G., 2006. Geothermal Disruption of Summit Glaciers at Mount Spurr Volcano, 2004-6: An Unusual Manifestation of Volcanic Unrest. U. S. Geological Survey Professional Paper 1732-B: 33.

Dixon, J.P., Stihler, S.D., Power, J.A., Tytgat, G., Estes, S., Prejean, S., Sanchez, J.J., Sanches, R., McNutt, S.R. and Paskievitch, J., 2005. Catalog of Earthquake Hypocenters at Alaskan Volcanoes: January 1 through December 31, 2004. USGS Open File Report 2005-1312.

Dixon, J.P., Stihler, S.D., Power, J.A., Tytgat, G., Moran, S.C., Sanchez, J., Estes, S., McNutt, S.R. and Paskievitch, J., 2003. Catalog of Earthquake Hypocenters at Alaskan Volcanoes: January 1 through December 31, 2002. USGS Open File Report 03-267.

Doukas, M.P. and McGee, K.A., 2007. A compilation of gas emission-rate data from volcanoes of Cook Inlet (Spurr, Crater Peak, Rebout, Iliamna, and Augustine) and Alaska Peninsula (Douglas, Fourpeaked, Griggs, Mageik, Martin, Peulik, Ukinrek Maars, and Vemniaminof), Alaska from 1995-2006. U.S. Geological Survey Open-File Report 2007-1400.

Fournier, R.O., 1999. Hydrothermal Processes Related to Movement of Fluid From Plastic into Brittle Rock in the Magmatic-Epithermal Environment. Economic Geology, 94(8): 1193-1212.

Freeze, R.A. and Cherry, J.A., 1979. Groundwater. Prentice-Hall, Inc., Englewood Cliffs, NJ 07632, 604 pp.

Garchar, L., Wendlandt, R., Martini, B. and Owens, L., 2012. Geochemistry of a Sub-glacial Volcanic Hydrothermal System at Mount Spurr, Alaska, PROCEEDINGS, Thirty-Seventh Workshop on Geothermal Reservoir Engineering, Stanford University, Stanford, CA.

Ingebritsen, S.E. and Manning, C.E., 2010. Permeability of the continental crust: dynamic variations inferred from seismicity and metamorphism. Geofluids, 10: 193-205.

Jolly, A.D., Page, R.A. and Power, J., 1994. Seismicity and stress in the vicinity of Mount Spurr volcano, south central Alaska. Journal of Geophysical Research, 99(B8): 15,305-315,318.

Juhle, W. and Coulter, H., 1955. The Mt. Spurr eruption, July 9, 1953. Eos (American Geophysical Union Transactions), 36(2): 199-202.

Keith, T.E.C., Editor, 1995. The 1992 Eruptions of Crater Peak Vent, Mount Spurr Volcano, Alaska. USGS Survey Bulletin 2139: 220.

Koulakov, I., West, M. and Izbekov, P., 2013. Fluid ascent during the 2004-2005 unrest at Mt. Spurr inferred from seismic tomography. Geophys. Res. Lett., 40: 4579-4582.

Lemmon, E.W., McLinden, M.O. and Friend, D.G., 2011. Thermophysical Properties of Fluid Systems. In: P.J. Linstrom and W.G. Mallard (Editors), NIST Chemistry WebBook, NIST Standard Reference Database Number 69. National Institute of Standards and Technology, Gaithersburg, MD, 20899.

Moran, S.C., Newhall, C. and Roman, D.C., 2011. Failed magmatic eruptions: Late-stage cessation of magma ascent. In: Moran SC, Newhall CG, Roman DC (eds) Failed eruptions: late-stage cessation of magma ascent. Bull Volcanol, 73(2): 115-122.

Motyka, R.J. and Nye, C.J., 1993. Fumarolic gas chemistry (1982) and thermal spring water chemistry, crater peak (1985), Mount Spurr, Alaska. Short Notes on Alaskan Geology, Alaska Department of Geological and Geophysical Survey Professional Report 113.

Neal, C.A., Coombs, M., Wessels, R. and McGimsey, R.G., 2007. Volcanic Disruption of Summit Ice at Mount Spurr Volcano, Alaska, 2004-2007, GSA Cordilleran Section - 103rd Annual Meeting (4-6 May 2007). GSA, Bellingham, WA.

Nye, C.J. and Turner, D.L., 1990. Petrology, geochemistry, and age of the Spurr volcanic complex, eastern Aleutian arc. Bull Volcanol, 52(3): 205-226.

Phillips, O.M., 1991. Flow and Reactions in Permeable Rocks. Cambridge University Press, New York.

Power, J., 2004. Renewed Unrest at Mount Spurr Volcano, Alaska. Eos (American Geophysical Union Transactions), 85(43).

Power, J.A., Stihler, S.D., Dixon, J.P., Moran, S.C., Caplan-Auerbach, J., Prejean, S.G., McGee, K., Doukas, M.P. and Roman, D.C., 2004. Renewed Seismic Unrest at Mount Spurr Volcano, Alaska in 2004: Evidence for a Magmatic Intrusion, American Geophysical Union, Fall Meeting 2004, pp. Abstract S51A-0143.

Power, J.A., Villasenor, A. and Benz, H.M., 1998. Seismic image of the Mount Spurr magmatic system. Bull Volcanol, 60: 27-37.

Riehle, J.R., 1985. A reconnaissance of the major Holocene tephra deposits in the upper Cook Inlet region, Alaska. Journal of Volcanology and Geothermal Research, 26(1-2): 37-74.

Schaefer, J.R., Coombs, M.L., Scott, W.E. and Neal, C.A., 2012. Recent non-eruptive, geothermal disruption of summit glaciers and resulting flow hazards at Mount Chiginagak and Mount Spurr volcanoes, Alaska, Volcano-Ice Interactions on Earth and Other Planets Conference III, Anchorage, Alaska.

Turner, D.L. and Wescott, E.M., 1986. Geothermal Energy Resource Investigations at Mt. Spurr, Alaska. Geophysical Institute of the University of Alaska.

Waythomas, C.F. and Nye, C.J., 2002. Preliminary Volcano-Hazard Assessment for Mount Spurr Volcano, Alaska. U.S. Geological Survey Open-File Report 01-482.

Werner, C.A., Doukas, M.P. and Kelly, P.J., 2011. Gas emissions from failed and actual eruptions from Cook Inlet Volcanoes, Alaska, 1989-2006. Bull Volcanol, 73(2): 155-173.

Appendix A: Symbol Definitions

Physical Meaning	Symbol	Value	Units
Latin Symbols			
Coefficient of pressure diffusivity	A	~2	m/s
Effective diffusivity	a^*	7×10^{-7}	m^2/s
Area	A		m^2
Speed of sound in water	c_1	1.4×10^3	m/s
Specific heat capacity of ice	c_i	2.11×10^3	J/kg ^oC
Specific heat capacity of andesite	c_a	1.4×10^3	J/kg ^oC
Specific heat capacity of $CO_2$200 to1000 ^oC	c_{CO2}	$1.2x\ 10^3$	J/kg ^oC
Specific heat capacity of water	c_w	4.2×10^3	J/kg ^oC
Thermal Energy	E		J
Acceleration due to gravity	G	9.8	m/s^2
Thickness of a hydrothermal system	H		m
Heat output	H		W
Permeability	K		m^2
Latent heat of fusion, H_2O	L_{wi}	3.4×10^5	J/kg
Length from impermeable barrier to hydrothermal sys.	L		m
Mass	M		kg
Pressure	P		Pa or bar
Mass flux	Q		kg/s or t/d
Rayleigh number	Ra		dimensionless
Rayleigh number, final	Ra_f		dimensionless
Rayleigh number, initial	Ra_i		dimensionless
A change in temperature	ΔT		^oC
Temperature, subscripts $_f$ is final, $_i$ is initial	T		^oC
Temperature of fusion, H_2O	T_{fus}	0	^oC
Initial temperature of magma	T_m	1000	^oC
Duration of event	T		s
Velocity of heat transport	U		m/s
Volume of melted ice, (Coombs *et al.*, 2006)	V_i	$\sim 5.4 \times 10^6$	m^3
Greek Symbols			
Thermal expansion coefficient, hydrothermal fluid	A	1.0×10^{-3}	$1/^oC$
Thickness of thermal conduction layer, final	δ_f		m
Thickness of thermal conduction layer, initial	δ_i		m
Thermal conductivity, andesite	Λ	2.9	W/m ^oC
Kinematic viscosity of hydrothermal fluid	N	3.0×10^{-7}	m^2/s
Density of Andesite	ρ_a	2.7×10^3	kg/m^3
Density of H_2O, scale analysis value	ρ_w	1.0×10^3	kg/m^3
Time scale of diffusion	τ_p		s
Porosity	Φ		dimensionless

Appendix B: A Derivation of a Boundary Layer Relationship to a Perturbation in Rayleigh Number

A steady-state hydrothermal system reacts to a perturbation from below. In this case, magma is emplaced below a hydrothermal system; outgassed volatiles from the emplaced magma provide additional heat to the base of a hydrothermal system, altering that hydrothermal system's behavior.

A hydrothermal system state can be described by its Rayleigh number, *Ra*:

$$Ra = \frac{\alpha g k T h}{\upsilon a^*} \quad [B1]$$

which indicates the vigor with which it convects. When the factors that determine the Rayleigh change, that change is reflected in the Rayleigh number and may be expressed as a ratio of the final Rayleigh number to the initial Rayleigh number.

$$\frac{Ra_f}{Ra_i} \quad [B2]$$

Any heat output by a volcanic hydrothermal system must then travel through a thermal boundary layer before being sensed at the surface. A hydrothermal system without proper vigor may be unable to transport heat at a rate sufficient enough to be sensed at the surface, such as in the case of melting glacial ice and snow on the volcanic surface.

However, changes in those factors which increase the Rayleigh number will increase the rigor with which the hydrothermal system convects, and in some cases be raised enough to transport heat across that thermal boundary layer to the surface. This thermal boundary layer is denoted as δ, which is related to the Rayleigh number by the scaling relationship:

$$\delta = \frac{h}{Ra} \quad [B3]$$

where it is shown that the boundary layer, δ, has an inverse relationship with *Ra*.

$$\delta \propto \frac{1}{Ra} \quad [B4]$$

An increase in Rayleigh number, Ra, expressed as a ratio of the final Rayleigh number, Ra_f, to the initial Rayleigh number, Ra_i, is then the inverse ratio of that which the final boundary layer, δ_f, is to the initial boundary layer, δ_i.

$$\frac{Ra_f}{Ra_i} = \frac{\delta_i}{\delta_f} \rightarrow \frac{Ra_f}{Ra_i}\delta_f = \delta_i \quad [B5]$$

The time lapse, t, is determined by the time change from the initiation of the thermal impulse, taken in this case to be the date of the initial seismic swarm, and the date which the thermal impulse was felt on the surface, denoted by the melting of ice.

Since we are interested in the change in boundary layer thickness, $\Delta\delta$, as it diminishes from its larger initial distance, δ_i, to its shorter final distance, δ_f, I assume that the time t needed to move the boundary a distance $\Delta\delta$ is given by

$$t = \frac{\delta_i - \delta_f}{u_f} \quad [B6]$$

The final velocity, u_f, is related to the final boundary layer, δ_f, and the effective diffusivity of the system, a^*, through scale analysis:

$$u_f = \frac{a^*}{\delta_f} \quad [B7]$$

Substituting [B7] into [B6] yields:

$$t = \frac{\delta_f}{a^*}\left(\delta_i - \delta_f\right) \quad [B8]$$

Multiply both sides by a^*:

$$a^* t = \delta_f\left(\delta_i - \delta_f\right) \quad [B9]$$

Substitute [B5] into [B9] for δ_i:

$$a^* t = \delta_f\left(\frac{Ra_f}{Ra_i}\delta_f - \delta_f\right) \quad [B10]$$

Factor out δ_f from the right side of the equation:

$$a^* t = \delta_f^2 \left(\frac{Ra_f}{Ra_i} - 1\right) \quad \text{[B11]}$$

Divide both sides by: $\left(\frac{Ra_f}{Ra_i} - 1\right)$

$$\frac{a^* t}{\left(\frac{Ra_f}{Ra_i} - 1\right)} = \delta_f^2 \quad \text{[B12]}$$

Take the square root of both sides:

$$\sqrt{\frac{a^* t}{\left(\frac{Ra_f}{Ra_i} - 1\right)}} = \delta_f \quad \blacksquare \quad \text{[B13]}$$